A B-Dot Acquisition Controller for the RADARSAT Spacecraft

Thomas W. Flatley, Wendy Morgenstern, Alan Reth, Frank Bauer
Code 712/Guidance, Navigation and Control Branch
Goddard Space Flight Center
Greenbelt, Maryland, 20904, USA

Abstract:
B-Dot is an extremely simple control law sometimes used for despinning satellites. It relies on magnetic coils or torque rods as control actuators. The control law is based on the measurement of the rate of change of body-fixed magnetometer signals. Using only a magnetometer and a magnetic moment generator, the B-Dot controller despins the spacecraft relative to the Earth's magnetic field vector. When the spacecraft carries a constant speed momentum wheel, B-Dot control will precess the wheel spin axis to the orbit normal.

The Canadian Space Agency's RADARSAT spacecraft is an Earth pointing, momentum bias system in a sun synchronous, dawn/dusk orbit. Its uses a passive Safehold Mode, relying on the momentum bias to maintain the spacecraft in a power positive state. This spacecraft presents an ideal opportunity for using B-Dot as an Sun Acquisition controller. It is an active controller, but it requires only magnetometers, magnetic torquers, and a momentum wheel, and the control law is very simple. This paper consists of two sections. The first presents a brief primer concerning a variety of magnetic controllers. The second section documents analysis and simulation results for the performance of the RADARSAT system using a B-Dot sun acquisition controller.

Introduction

We will be discussing an attitude control concept which has been frequently applied to low Earth orbit spacecraft, usually for despinning or unloading unwanted spacecraft angular momentum. A key ingredient in the B-Dot controller is the rate of change of magnetic field vector components as measured by on-board, body-fixed sensors called magnetometers. "B" is commonly used to denote the Earth's magnetic field, and the associated rate of change $^{dB}/_{dt}$, is often written $\dot{B}$. Thus, the term "B-Dot."

The actuators used in such systems are magnetic coils or torque rods. Both types of actuators produce magnetic moments which interact with the Earth's magnetic field to generate external torques on the spacecraft. The effect is calculated by the expression $\vec{T} = \vec{M} \times \vec{B}$. In SI units, the torque, $\vec{T}$, in N-m equals the cross product of the magnetic moment, $\vec{M}$, in amp-m^2 with the magnetic field, $\vec{B}$, in tesla.

With air core magnetic coils, the magnetic moment is simply the current through the coil, measured in amperes, times the area of the coil in m^2 times the number of loops in the coil. Torque rods, on the other hand, are usually long and slender, with many turns of wire wound on a cylindrical rod made of highly permeable material. The magnetic properties of the solid core dramatically amplify the magnetic moment produced by the current loops at the expense of additional weight.

Section 1: A Brief Survey of Magnetic Controllers.

1.1 B-Dot Control

In general, B-Dot control laws command, on a per-axis basis, a magnetic moment whose sign is opposite to that of the rate of change of the magnetic field along that axis.

1.1 .1 B-Dot Proportional Control

For a typical spacecraft axis, we set $M_X = -k \dot{B}_X$ for a magnetometer and a torquer aligned with the X-axis of the spacecraft, where k is a positive constant, M_X is the commanded dipole for the X-axis torquer, and B_X is the component of the Earth's magnetic field along the X-axis.

Let us apply this proportional control to the simple example depicted in Figure 1: Consider a body spinning about its Z-axis, with a moment of inertia, I_z, and a spin rate, ω_z. Let the Earth's magnetic field vector be in the X-Y plane, with a magnitude B_o. A single-axis magnetometer is aligned with X, and measures the B_x component of $\vec{B}$. Our example also includes a magnetic torquer, along the X-axis.

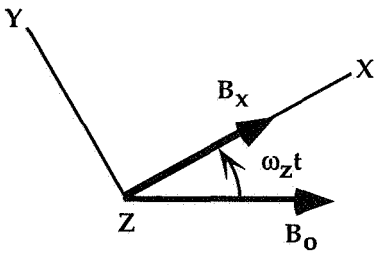

Figure 1: Geometry for Example

From this geometry, note that $B_x = B_o \cos\omega_z t$, so that $\dot{B}_x = -B_o\omega_z \sin\omega_z t$. Initial phase angle is take as zero, without loss of generality. Using the proportional control law suggested above we have a commanded dipole of

$$M_x = -k\dot{B}_x = k B_o\omega_z \sin\omega_z t$$

for the X-axis torquer. Because of the convenient geometry of this example, $\vec{M}\times\vec{B}$ will be a vector in the Z direction, with $T_z = M_x B_y$.

The geometry shows that $B_y = -B_o \sin\omega_z t$. We thus have

$$T_z = (kB_o\omega_z \sin\omega_z t)(-B_o \sin\omega_z t)$$

$$T_z = -kB_o^2\omega_z \sin^2\omega_z t$$

Over one revolution, the average value of $\sin^2\omega_z t$ will be 0.5, so the average torque generated by the proportional controller using one torquer will be: $T_{z,ave} = \frac{-kB_o^2\omega_z}{2}$.

Basic physics tells us that the rate of change of angular momentum equals the torque applied. In this example, a body spinning about its Z-axis, the angular momentum, H_z, is given by $I_z\omega_z$. Its derivative is then:

$$I_z\dot{\omega}_z = \dot{H}_z = T_{z,ave} = \frac{-kB_o^2\omega_z}{2}$$

This equation may be rewritten:

$$\dot{\omega}_z + \frac{kB_o^2}{2I_z}\omega_z = 0$$

and is of the form, $\dot{\omega}_z + \frac{\omega_z}{\tau} = 0$ where τ is a decay time constant. The solution of this equation is $\omega_z = \omega_{z_o} e^{-t/\tau}$ with $\tau = \frac{2I_z}{kB_o^2}$ and ω_{z_o} the initial spin rate. From this solution, we see that the controller causes the spin rate to decay exponentially.

If a second magnetic torque is applied along the Y-axis, we would then have the additional term $\dot{B}_y = -B_o\omega_z \cos\omega_z t$ resulting in a commanded Y-axis dipole of $M_y = -k\dot{B}_y = kB_o\omega_z \cos\omega_z t$. With this additional control authority, the resultant torque becomes:

$$T_z = M_x B_y - M_y B_x$$

$$T_z = (kB_o\omega_z \sin\omega_z t)(-B_o \sin\omega_z t) - (kB_o\omega_z \cos\omega_z t)(B_o \cos\omega_z t)$$

$$T_z = -kB_o^2\omega_z$$

$$T_z = -kB_o^2\omega_z = \dot{H}_z = I_z\dot{\omega}_z$$

which leads to the equation:

$$\dot{\omega}_z + \frac{kB_o^2\omega_z}{I_z} = 0.$$

This yields the same form of solution, $\omega_z = \omega_{z_o} e^{-t/\tau}$, but with a different time constant, $\tau = \frac{I_z}{kB_o^2}$. Comparing this to the time constant for control with the single, X-axis torquer, we see that adding the Y-axis control cuts the time constant for the spin decay in half.

Now consider the maximum allowable value for k consistent with proportional control and a finite torquer capacity. This is tantamount to setting $kB_o\omega_z = M_o$, where M_o is the maximum torquer dipole. At this maximal k value, the T_z using two torquers, becomes

$$T_{z,max} = -M_oB_o$$

This maximal estimate provides a useful benchmark for comparison to the effects of the B-Dot bang-bang controller described in the next section.

1.1.2 B-Dot Bang-Bang Control:

As an alternative to the proportional B-Dot controller, consider a bang-bang system where, instead of using proportional control to calculate the dipole command, the maximum torquer strength is always used. Let

$$M_x = -M_o\,\mathrm{sgn}\left(\dot{B}_x\right) = \begin{cases} -M_o \text{ if } \dot{B}_x > 0 \\ M_o \text{ if } \dot{B}_x < 0 \end{cases} \quad \text{and similarly,} \quad M_y = -M_o\,\mathrm{sgn}\left(\dot{B}_y\right) = \begin{cases} -M_o \text{ if } \dot{B}_y > 0 \\ M_o \text{ if } \dot{B}_y < 0 \end{cases}$$

where "sgn" stands for "sign of" and M_o is the maximum torquer dipole. Then,

$$T_z = M_xB_y - M_yB_x = \left(-M_o\,\mathrm{sgn}\,\dot{B}_x\right)\left(-B_o\sin\omega_z t\right) - \left(-M_o\,\mathrm{sgn}\,\dot{B}_y\right)\left(B_o\cos\omega_z t\right)$$

$$T_z = M_oB_o\left[\mathrm{sgn}\left(-B_o\omega_z\sin\omega_z t\right)\sin\omega_z t + \mathrm{sgn}\left(-B_o\omega_z\cos\omega_z t\right)\cos\omega_z t\right]$$

For $B_o, \omega_z > 0$,

$$\mathrm{sgn}\left(-B_o\omega_z\sin\omega_z t\right) = -\mathrm{sgn}\left(\sin\omega_z t\right)$$

$$\mathrm{sgn}\left(-B_o\omega_z\cos\omega_z t\right) = -\mathrm{sgn}\left(\cos\omega_z t\right)$$

Thus, T_z will be given by the sum of rectified sine and cosine functions. The average value of a rectified sine or cosine wave is $2/\pi$, so the average value of the torque generated by each actuator is $-\frac{2}{\pi}M_oB_o$. With two torquers, the average torque generated is:

$$T_{z,ave} = -\tfrac{4}{\pi}M_oB_o.$$

Note that the proportional control has a $T_{z,max} = -M_oB_o$. In comparison, the bang-bang controller raises the resultant torque by a factor of $\frac{4}{\pi}$, a 27% increase.

Equating the average torque to the rate of change of angular momentum we have:

$$I_z\dot{\omega}_z = -\tfrac{4}{\pi}M_oB_o$$

From the solution of this equation, we see that we have a linear spin rate decay given by

$$\omega_z = \omega_{z_o} - \frac{4}{\pi}\frac{M_oB_o}{I_z}t$$

which is faster than the exponential decay resulting from proportional B-dot control described in the last section.

1.2 $\vec{H}\times\vec{B}$ Momentum Unloading Controller

It is of interest to contrast the B-Dot control described here to the performance of an $\vec{H}\times\vec{B}$ law which is another magnetic controller often used for spacecraft momentum unloading and despin.

1.2.1 $\vec{H}\times\vec{B}$ Control, Single Axis Example

Let $\vec{M} = k\left(\vec{H}\times\vec{B}\right)$ where $\vec{H}$ is the angular momentum vector and k is an arbitrary constant. Since $\vec{T} = \vec{M}\times\vec{B}$, we have:

$$\vec{T} = k\left(\vec{H}\times\vec{B}\right)\times\vec{B}$$

$$\vec{T} = k\left[\left(\vec{H}\cdot\vec{B}\right)\vec{B} - B^2\vec{H}\right]$$

Applying this control law to our simple example, we see $\vec{H}\cdot\vec{B} = 0$, since $\vec{H}$ is perpendicular to $\vec{B}$ and $B^2 = B_o^2$.

Since $\dot{\vec{H}} = \vec{T}$, we have: $\qquad \dot{\vec{H}} = -kB_o^2\vec{H}$

Or, rearranging: $$\dot{\vec{H}} + kB_0^2\vec{H} = 0$$

Since in our example $\vec{H}$ has only a Z-component, which is given by $I_z\omega_z$, this equation becomes:

$$\dot{\omega}_z + kB_0^2\omega_z = 0$$

giving us an exponential spin rate decay with a time constant of:

$$\tau = \frac{1}{kB_0^2}$$

Compare this to the exponential decay seen with the proportional B-Dot control, where the time constant was calculated to be $\tau = \frac{I_z}{kB_0^2}$. Both controllers produce exponential decay with time constants inversely proportional to the control gain and the square of the available magnetic field strength. This highlights the fact that, for momentum unloading, B-Dot control is qualitatively identical to $\vec{H} \times \vec{B}$ control.

1.2.2 Three-Axis $\vec{H} \times \vec{B}$ Control

To round out our primer on magnetic controllers, this section is included as a brief aside, extending $\vec{H} \times \vec{B}$ beyond our simple example, to the general three-axis case.

In the general case of $\vec{H} \times \vec{B}$ control, consider: $$\dot{\vec{H}} = k\left[(\vec{H}\cdot\vec{B})\vec{B} - B^2\vec{H}\right]$$

Taking the dot product of both sides with $\vec{H}$: $$\vec{H}\cdot\dot{\vec{H}} = k\left[(\vec{H}\cdot\vec{B})(\vec{H}\cdot\vec{B}) - B^2\vec{H}\cdot\vec{H}\right]$$

This can be written:

$$\frac{1}{2}\frac{d}{dt}(\vec{H}\cdot\vec{H}) = k\left[(\vec{H}\cdot\vec{B})^2 - B^2(\vec{H}\cdot\vec{H})\right]$$

$$\frac{1}{2}\frac{d}{dt}(H^2) = k\left[(HB\cos\theta)^2 - H^2B^2\right]$$

where θ is the angle between $\vec{H}$ and $\vec{B}$ and H is the magnitude of $\vec{H}$.

Continuing on,

$$H\dot{H} = kH^2B^2(\cos^2\theta - 1)$$

$$\dot{H} = -kB^2H\sin^2\theta$$

From this, it can be seen that the magnitude of $\dot{H}$ is never greater than zero, so the angular momentum is monotonically non-increasing.

For our example, with $\vec{H}$ perpendicular to $\vec{B}$ and magnitude of $\vec{B}$ equal to B_0, this expression reduces to,

$$\dot{H} = -kB_0^2H$$

a result in agreement with that shown in the previous section on $\vec{H} \times \vec{B}$.

Section 2: Possible Application of B-Dot as a RADARSAT Sun Acquisition Mode

In the ensuing discussion, Safehold Mode refers to the passive Safehold Mode, currently in use on-board the RADARSAT spacecraft. B-Dot Sun Acquisition is the authors' proposed controller, a bang-bang B-Dot control law.

2.1 Spacecraft Description

RADARSAT is a Canadian satellite launched into an 800 km altitude circular, sun-synchronous, dusk-dawn orbit in January 1996. In this orbit, the spacecraft is in full sun for approximately ten contiguous months of the year, but there is a two month season during which eclipses occur once per orbit. For RADARSAT, the eclipse season is centered around the time of summer solstice, approximately June 20, when the sun is about 32° north of the orbit normal. At this time, the solar array illumination is at a minimum, about 85% of peak when the spacecraft is in sunlight, and the spacecraft flies through the Earth's shadow in the south polar regions, further reducing the average power available.

Figure 2 shows a sketch of the RADARSAT spacecraft in its normal operational configuration. The $+X_c$ (roll) axis is nominally aligned with the velocity vector. The solar arrays face orbit normal, and the $+Z_c$ axis (yaw) points down, toward the Earth. Here, the "c" subscript refers to the "control" axes.

The spacecraft has two pairs of Y and Z axes, "mechanical" and "control." The mechanical axes are aligned with the body cube, while the control axes are aligned with the desired science attitude. The solar arrays face in the negative Y_c direction. The Synthetic Aperture Radar (SAR) looks out in the $+Z_m$ direction. To meet the science requirements, the SAR should be "rolled" 30° away from the nadir direction. This places the $+Z_c$ and the $+Z_m$ axes 30° apart, as shown in Figure 3.

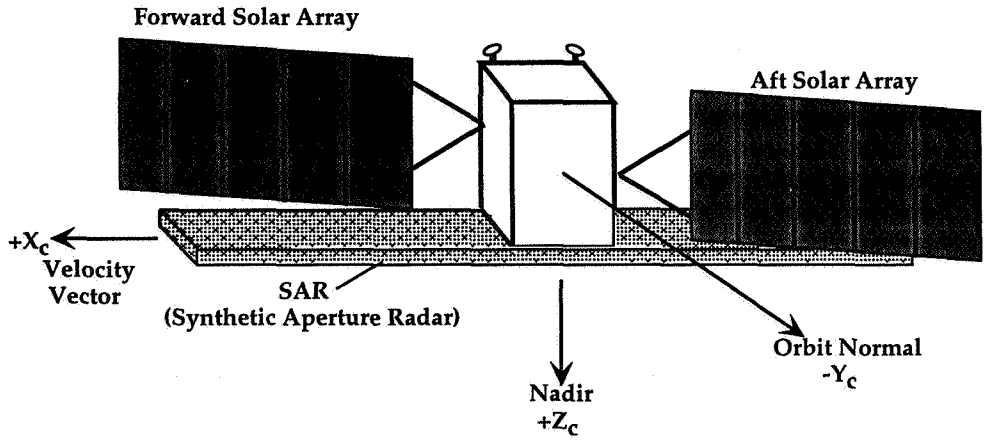

Figure 2: RADARSAT, Normal Operational Configuration

The spacecraft has a momentum wheel aligned with the Y_c axis and reaction wheels on the X_c and Z_c axes. The momentum wheel provides a momentum bias for the system along the orbit normal. Typically, such a bias is used for passive roll/yaw control on an Earth-pointed spacecraft, but the RADARSAT controller is designed so that gyroscopic coupling is thwarted, and the control closely resembles that of a three-axis, zero momentum system. This approach creates three uncoupled single-axis control channels, simplifying the controller design.

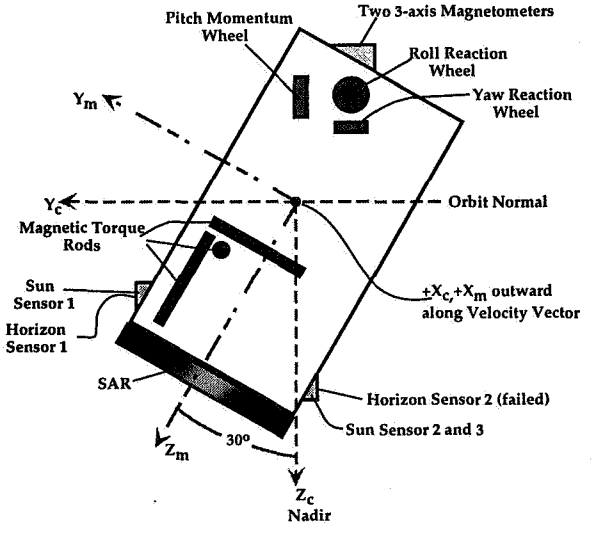

Figure 3: RADARSAT ACS Hardware

The intent of the pitch momentum bias on RADARSAT is to provide a passive Safehold Mode for the spacecraft. Its Safehold Mode, which is entered automatically in the event of a problem, simply disables all active control and sheds all non-essential loads. The momentum wheel runs down, transferring its angular momentum to the spacecraft body. The body spins up causing it to remain pointed approximately along the orbit normal, where orbit normal is approximately equal to the sunline. This places RADARSAT in a thermal and power safe condition. The solar arrays continue to receive near-nominal illumination. However, Y_c is not a principal axis, so the spin-up produces a very complex motion.

The performance of such a passive Safehold Mode is extremely sensitive to initial conditions at the time of entry. During the first eclipse season in the summer 1996, a series of spacecraft anomalies resulted in a transition to Safehold Mode under less than ideal initial conditions. The ensuing spacecraft motion led to a severe power shortage which almost resulted in a loss of mission.

2.2 Normal Equilibrium State

In its normal mode of operation, the spacecraft rotates at the orbit rate, ω_o about the $-Y_c$ axis. The momentum wheel provides a bias of 50 Nms in the same direction. Because of significant products of inertia about the controller axes, the resultant spacecraft angular momentum vector, $\vec{H}$, is not along the orbit normal in this state and potential nutation problems exist. The reaction wheels, however, can be run at bias speeds which places the system momentum vector along the $-Y_c$ axis.

Consider

$$H_x = I_{xx}\omega_x - I_{xy}\omega_y - I_{xz}\omega_z + h_{rw,x}$$
$$H_z = -I_{xz}\omega_x - I_{yz}\omega_y + I_{zz}\omega_z + h_{rw,z}$$

where: H_x, H_y, H_z are the angular momentum components
$\omega_x, \omega_y, \omega_z$ are the angular velocity components
$h_{rw,x}$, $h_{rw,y}$, $h_{rw,z}$ are the wheel momenta.

We want $H_x = H_z = 0$ when $\omega_x = \omega_z = 0$ and $\omega_y = -\omega_o$. It follows that we require:

$$I_{xy}\omega_o + h_{rw,x} = 0$$
$$I_{yz}\omega_o + h_{rw,z} = 0$$

Thus, if the roll reaction wheels runs with a momentum of $h_{rw,x} = -I_{xy}\omega_o$ and the yaw wheel runs with $h_{rw,z} = -I_{yz}\omega_o$, the spacecraft rotation about the -Y_c axis will represent an equilibrium state.

Entering the proposed B-Dot Sun Acquisition Mode from a nominal state would involve the initial conditions:

$\omega_x = 0$ $\quad h_{rw,x} = -I_{xy}\omega_o \approx$ -2 Nms
$\omega_y = -\omega_o$ $\quad h_{rw,y} = -50$
$\omega_z = 0$ $\quad h_{rw,z} = -I_{yz}\omega_o \approx$ -1 Nms

These initial conditions are assumed in all of the simulations results presented in Section 2.4.

2.3 Simulations

From the magnetic controllers discussed in section one, the authors chose a three-axis bang-bang B-Dot controller for its speed, and simplicity. It can also takes advantage of the maximum available control authority, by setting the commanded dipole to the torquer's limit, although none of our simulations depict this situation. This controller, used in conjunction with a constant speed pitch momentum wheel, will precess the wheel spin axis to orbit normal. Performance was evaluated using RADARSAT mass properties in a FORTRAN simulation of the spacecraft dynamics and kinematics.

Spacecraft dynamics were modeled by the three classical Euler equations[2]:

$$\dot{H}_x + \omega_y H_z - \omega_z H_y = T_x$$
$$\dot{H}_y + \omega_z H_x - \omega_x H_z = T_y$$
$$\dot{H}_z + \omega_x H_y - \omega_y H_x = T_z$$

T_x, T_y, T_z are components of the external torques

Classical quaternion equations were integrated to model the kinematics[2]:

$$\dot{q}_1 = \tfrac{1}{2}\left(\omega_z q_2 - \omega_y q_3 + \omega_x q_4 \right)$$
$$\dot{q}_2 = \tfrac{1}{2}\left(-\omega_z q_1 + \omega_x q_3 + \omega_y q_4 \right)$$
$$\dot{q}_3 = \tfrac{1}{2}\left(\omega_y q_1 - \omega_x q_2 + \omega_z q_4 \right)$$
$$\dot{q}_4 = \tfrac{1}{2}\left(-\omega_x q_1 - \omega_y q_2 - \omega_z q_3 \right)$$

The spacecraft attitude matrix, [A], was obtained from the quaternion elements from[2]:

$$[A] = \begin{bmatrix} q_1^2 - q_2^2 - q_3^2 + q_4^2 & 2(q_1q_2 + q_3q_4) & 2(q_1q_3 - q_2q_4) \\ 2(q_1q_2 - q_3q_4) & -q_1^2 + q_2^2 - q_3^2 + q_4^2 & 2(q_2q_3 + q_1q_4) \\ 2(q_1q_3 + q_2q_4) & 2(q_2q_3 - q_1q_4) & -q_1^2 - q_2^2 + q_3^2 + q_4^2 \end{bmatrix}$$

The nature of the RADARSAT orbit allows a very simple representation of the orbital motion. It was assumed that the orbit was inertially fixed, with the ascending node and the Earth's North Pole defining an inertial reference frame. Actually, the orbit moves at about one degree per day, keeping up with the motion of the sun, but for the short simulations described here, this effect has been ignored. Figure 4 shows the orbital representation and the spacecraft position vector components used. Axis 1 aligns with the ascending node, axis 3 corresponds to the North Pole, and axis 2 completes the right-hand coordinate frame.

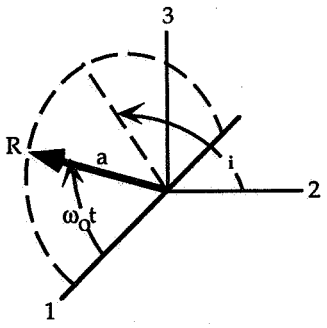

i = orbit inclination = 98.7°

a = orbit radius = $|\vec{R}|$

$\vec{R}$ is the spacecraft position vector, and $\vec{r}$ is the corresponding unit vector, $\vec{R}/a$

Let ω_o equal orbit rate. Then, we define,

$$R_1 = a\,r_1 = a(\cos\omega_o t) \qquad r_1 = \cos\omega_o t$$
$$R_2 = a\,r_2 = a(\sin\omega_o t\,\cos i) \quad \text{so} \quad r_2 = \sin\omega_o t\,\cos i$$
$$R_3 = a\,r_3 = a(\sin\omega_o t\,\sin i) \qquad r_3 = \sin\omega_o t\,\sin i$$

Figure 4: Orbital Elements

A tilted dipole model of the Earth's Magnetic field was used[2]. In the inertial frame, the field is given by:

$\vec{b} = B_o\left[\vec{m} - 3(\vec{m}\cdot\vec{r})\vec{r}\right]$ where B_o is field strength at the magnetic equator at the spacecraft altitude.

$\vec{m}$ is the unit vector along the dipole axis

$\vec{r}$ is the unit vector to the spacecraft position, with the components of $\vec{r}$, r_1, r_2, and r_3, as given above.

$\vec{m}$ is tilted 11° away from the North Pole and rotates with the Earth, so we let:

$$m_1 = \sin 11^\circ \cos\omega_E t$$
$$m_2 = \sin 11^\circ \sin\omega_E t \quad \text{where } \omega_E \text{ is Earth rate.}$$
$$m_3 = \cos 11^\circ$$

We define $\vec{B}$ as the magnetic field vector in body coordinates, so we have

$$\vec{B} = [A]\vec{b}$$

For B-Dot, we need the derivative of $\vec{B}$, which is given by

$$\dot{\vec{B}} = [A]\dot{\vec{b}} + [\dot{A}]\vec{b}$$
$$\dot{\vec{B}} = [A]\dot{\vec{b}} + [\dot{A}][A]^T\vec{B}$$

Rearranging,

$$\dot{\vec{B}} - [\dot{A}][A]^T\vec{B} = [A]\dot{\vec{b}}$$
$$\dot{\vec{B}} + [\Omega]\vec{B} = [A]\dot{\vec{b}}$$

Here, $[\Omega] = -[\dot{A}][A]^T$ is the cross product operator for the angular velocity, i.e. $\vec{\Omega} = \begin{pmatrix} 0 & -\omega_z & \omega_y \\ \omega_z & 0 & -\omega_x \\ -\omega_y & \omega_x & 0 \end{pmatrix}$.

The equation for $\dot{\vec{B}}$ can also be written

$$\dot{\vec{B}} + \vec{\omega}\times\vec{B} = [A]\dot{\vec{b}}$$
$$\dot{\vec{B}} = [A]\dot{\vec{b}} - \vec{\omega}\times\vec{B}$$

To get $\dot{\vec{b}}$, recall that $\vec{b} = B_o\left[\vec{m} - 3(\vec{m}\cdot\vec{r})\vec{r}\right]$

Then, $\dot{\vec{b}} = B_o\left[\dot{\vec{m}} - 3(\vec{m}\cdot\vec{r})\dot{\vec{r}} - 3\left(\vec{m}\cdot\dot{\vec{r}} + \dot{\vec{m}}\cdot\vec{r}\right)\vec{r}\right]$

with $\vec{m}$ and $\vec{r}$ as given above, and,

$$\dot{\vec{m}} = \begin{pmatrix} -\sin 11^\circ\omega_E \sin\omega_E t \\ \sin 11^\circ\omega_E \cos\omega_E t \\ 0 \end{pmatrix} \qquad \dot{\vec{r}} = \begin{pmatrix} -\omega_o \sin\omega_o t \\ \omega_o \cos i \cos\omega_o t \\ \omega_o \sin i \cos\omega_o t \end{pmatrix}$$

We take the external torque in the Euler equations to be that due to gravity gradient and magnetic torques. The first is given by

$$\vec{T}_{gg} = 3\omega_0^2 \hat{r} \times I\hat{r}$$

$$\hat{r} = [A]\vec{r}$$

where $\hat{r}$ is the position unit vector in body coordinates and I^1 is the spacecraft's inertia tensor:

$$I = \begin{bmatrix} I_{xx} & -I_{xy} & -I_{xz} \\ -I_{xy} & I_{yy} & -I_{yz} \\ -I_{xz} & -I_{yz} & I_{zz} \end{bmatrix} = \begin{bmatrix} 4495 & -1836 & 221 \\ -1836 & 16233 & -768 \\ 221 & -768 & 15319 \end{bmatrix} \text{kg - m}^2$$

The magnetic torques are simply $\vec{T} = \vec{M} \times \vec{B}$ where $\vec{M}$ is the magnetic moment generated by the controller and $\vec{B}$ is the magnetic field in body coordinates.

2.4 Simulation Results

The results of five simulations are described in this section. In all cases , the season was selected such that the sun was on the orbit normal; Wheels speeds were initially set to the values derived in Section 2.2; Body rates were set to zero for roll and yaw, and negative orbit rate along the pitch axis. In the first three cases, initial attitude matches the RADARSAT normal configuration described in Section 2.1, corresponding to zero attitude errors. In the last two cases, an initial attitude of 77° in pitch is assumed.

For each run, four variables are displayed in the following plots:

- The angle between the spacecraft pitch axis and the orbit normal, ideally zero.
- The spacecraft pitch angle, with the zero pitch corresponding to $+Z_c$ nadir pointing.
- The pitch wheel angular momentum.
- The spacecraft normalized power, defined as the cosine of the angle between the sunline and the solar array normal. Ideally, this is value is 100% indicated that the solar arrays perpendicular to the sunline.

The roll and yaw wheels were turned off at the start of each run, but their momentum histories are not plotted. In all of the simulations discussed here, they run down in less than 16 minutes due to coulomb and viscous friction, and remain off for all subsequent time. The first three simulations were run for a duration of 24 hours; the last two were run for approximate four and a half hours, or 16000 seconds.

2.4.1 Nominal RADARSAT Safehold Mode Entry

Run 1 begins with the spacecraft in its normal attitude with initial wheel speeds and body rates as described above. Then, the wheels were simply turned off. This represents the best case scenario for RADARSAT entering its passive Safehold Mode. The pitch wheel runs down in about 90 minutes, transferring its angular momentum to the main body. During that time, the pitch axis gradually drifts away from the orbit normal, ending up about 30° off by the time the wheel stops. The pitch angle plot shows that the spacecraft did spin up, to about four revolutions per orbit about the maximum axis of inertia. The power dropped about 15% in the equilibrium state. This state would be thermal and power-safe indefinitely. Gravity gradient torque acting on the spinning body will tend to keep the system angular momentum vector in the vicinity of the orbit normal as it moves along at 1° per day. These

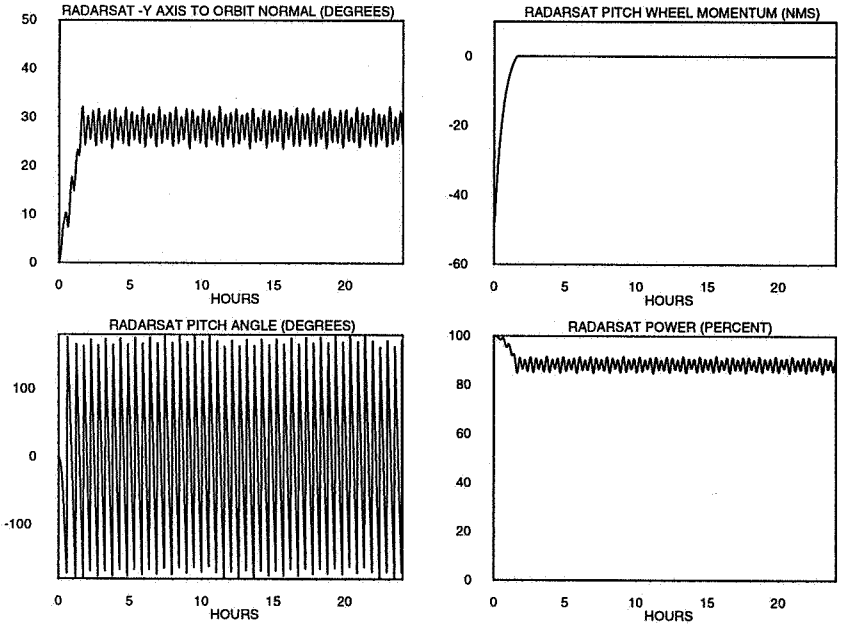

Figure 5: Nominal RADARSAT Safehold Mode Entry

torques precess the spin axis to keep up with the motion of the sun.
For nominal initial conditions, the RADARSAT Safehold Mode is acceptable. It is unforgiving, however, with respect to off-nominal initial conditions, as Section 2.4.4 demonstrates.

2.4.2 B-Dot Controller, Nominal Initial Conditions

This run shows how a bang-bang B-Dot controller using ±100 Amp-m^2 dipole levels would perform, assuming the same initial conditions as Run 1. The same variables are plotted, but note that now, the pitch wheel momentum is maintained at 50 Nms. The roll and yaw wheels still run down to zero. The pitch axis again moves away from the orbit normal, but now it wanders less than 10°. The pitch angle shows that the spacecraft initially begins to rotate with the Earth's magnetic field, about two revolutions per orbit inertially and one revolution per orbit relative to the local vertical. Near the end of the day, however, the combination of magnetic and gravity gradient torques results in gravity gradient capture indicated by the pitch angle settling to -90° , with $+X_c$ nadir pointing. Nearly full power is maintained during the entire run. This state would also be thermally and power safe indefinitely.

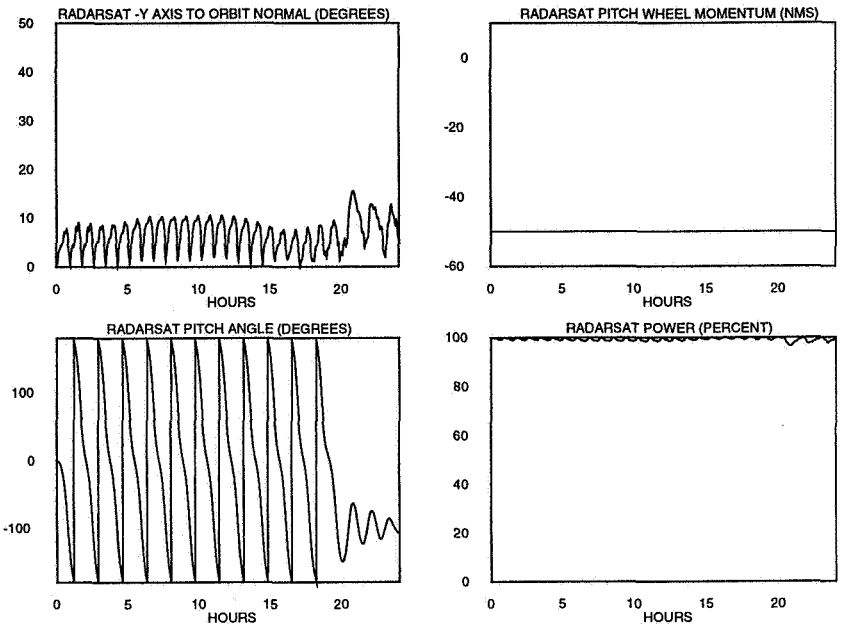

Figure 6: B-Dot Acquisition Controller, Nominal Initial Conditions

2.4.3 Nominal Safe Mode and B-Dot

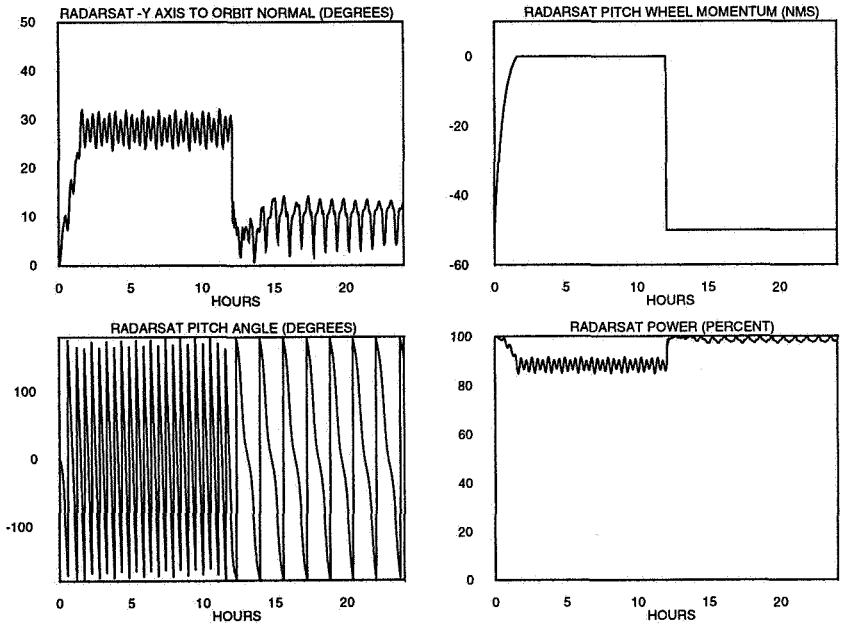

In Run 3, we repeat the first twelve hours of Run 1, the passive Safehold Mode case, then switch to the B-Dot control, as proposed for Run 2. Note the pitch wheel momentum decaying to zero, then going back up to 50 Nms at the twelve hour mark. The pitch axis quickly moves much closer to the orbit normal, the spin of the spacecraft slows down as shown by the pitch angle plot, and the power jumps to near 100% the B-Dot Sun Acquisition control scheme is initiated.

Figure 7: Nominal B-Dot Acquisition Mode

2.4.4 Passive Safehold Performance with Initial Pitch Angle of 77°

On Day 171 of 1996, the RADARSAT spacecraft entered Safehold with an initial pitch angle of 77°. Figure 8 shows the results of a Ball Aerospace simulation of the attitude motion which occurred. This data was presented at the RADARSAT ACS Evaluation Team (AET) Kickoff meeting in September, 1996. Of particular interest are the plots of the pitch and yaw angles. The first shows that the spacecraft entered a gravity gradient capture mode rather than spinning up around the pitch axis as it would have with more nominal initial conditions. As the pitch wheel spun down, gravity gradient torques on the body dumped the angular momentum that was intended to provide gyroscopic attitude stability in Passive Safehold. The yaw angle plot shows the worst effect. With no yaw stability in the gravity gradient mode, the spacecraft turned away from the sun and the solar arrays were no longer illuminated.

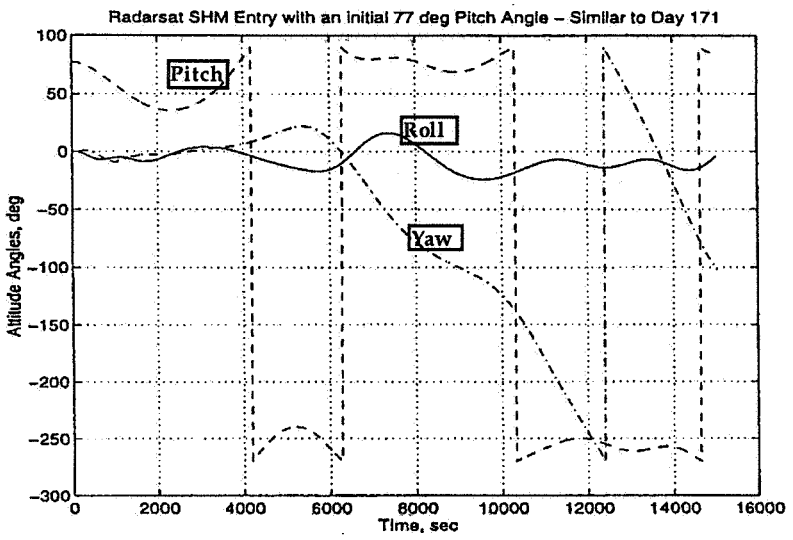

Figure 8: Ball Simulation of RADARSAT Safehold Emergency

This run, Figure 9, shows the results of the authors' simulation of this scenario. The run time of 16000 seconds was selected to facilitate easy comparison with the Ball results. The test began with nominal rates and zero roll and yaw angles. The only off-nominal initial condition was the 77° pitch angle. The pitch angle history closely matches that shown in the previous figure. Due to yaw motion, the angle between the spacecraft pitch axis and the orbit normal plot shows the 180° shift which turned the arrays backside to the sun. Also shown however is a power plot which reveals the seriousness of the situation which occurred.

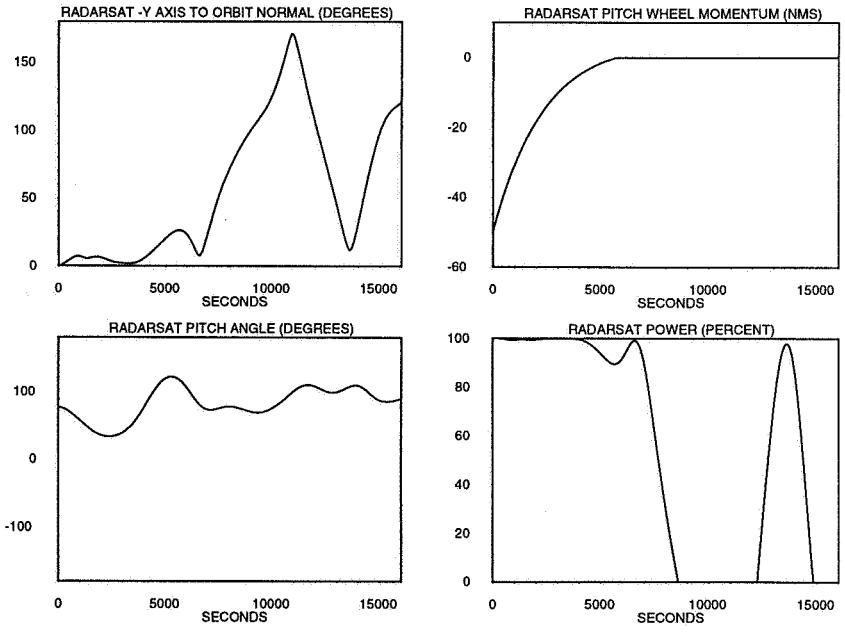

Figure 9 : Passive Safehold Performance, High Initial Pitch Angle

2.4.5 B-Dot Sun Acquisition with Initial Pitch Angle of 77°

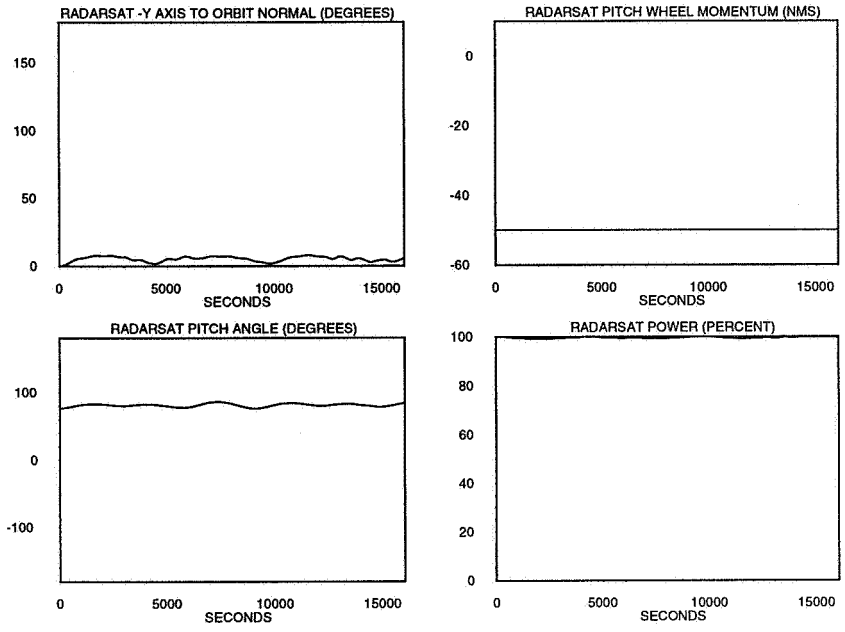

Figure 10: Proposed B-Dot Sun Acquisition , High Initial Pitch Angle

This simulation demonstrates the spacecraft attitude behavior for the proposed B-Dot Sun Acquisition controller given the same initial condition described in the last section, 2.4.4. A ± 100 A-m^2 torque level is used with the bang-bang controller. When considering the performance, note that this is not the maximum possible dipole. Control authority could be increased, by raising the commanded dipole level to the hardware limit ± 500 A-m^2.

Again, gravity gradient capture occurs, but here the -Y axis stays in the vicinity of the orbit normal, which corresponds to the sunline for the simulated season, and the solar arrays continue to produce full power. With the pitch wheel continuing to run, the system has gyroscopic roll/yaw stability which maintains the safe power and thermal conditions.

Conclusions

The passive Safemode is an acceptable strategy, given favorable initial conditions. However, it is not robust against all possible perturbations of the initial conditions, as demonstrated by the July 1996 emergency. The B-Dot Acquisition scheme examined in this paper is particularly suited to the RADARSAT system. The orbital properties are ideal for the success of B-Dot as an acquisition controller; the control law itself is extremely simple to implement; and it requires a minimal set of the available on-board sensors and actuators. Lastly, the proposed B-Dot scheme is robust against off nominal initial conditions, such as the high entry angle that resulted in the Safehold Mode emergency in July of 1996.

References:

1. RADARSAT Bus User's Manual. RSINT-ML0015-B(DRAFT). July 17, 1996.

2. Wertz, James, ed. Spacecraft Attitude Determination and Control. Kluwer Academic Publishers. Boston. 1978.